Synthesis and Structure of Zirconium(IV) Complexes Stabilized by the Bis(amido−phosphine) Macrocycle $[P_2N_2]$ $\{[P_2N_2] = PhP(CH_2SiMe_2NSiMe_2CH_2)_2PPh\}$

Michael D. Fryzuk,* Jason B. Love, and Steven J. Rettig†

Department of Chemistry, University of British Columbia, 2036 Main Mall, Vancouver, British Columbia V6T 1Z1, Canada

Received September 10, 1997

The preparation and characterization of a series of zirconium(IV) complexes that incorporate the macrocyclic bis(amido−phosphine) ligand $PhP(CH_2SiMe_2NSiMe_2CH_2)_2PPh$, $[P_2N_2]$, are described. The starting material, $ZrCl_2[P_2N_2]$, is prepared by reaction of *syn*-$Li_2(S)[P_2N_2]$ (S = dioxane or THF) with $ZrCl_4L_2$ (L = THT, tetrahydrothiophene; L = THF, tetrahydrofuran). Subsequent replacement of the chloride ligands can be achieved to generate the dialkyl complexes $ZrR_2[P_2N_2]$ (R = Me, CH_2Ph). Reaction with "magnesium butadiene", $Mg(C_4H_6)\cdot 2THF$, results in the formation of π-η^4-butadiene complex $Zr(\eta^4\text{-}C_4H_6)[P_2N_2]$. In addition, the *tert*-butylimido complex $Zr(NBu^t)[P_2N_2]$ can be prepared by addition of $LiNHBu^t$ to $ZrCl_2[P_2N_2]$. A number of the above complexes have been characterized by X-ray crystallography, and all show that the Zr center sits above the plane defined by the donor atoms of the macrocyclic ligand. The distortions of the macrocyclic ring observed in the solid state are not evident in solution and suggest that these ligand backbones are considerably flexible.

Introduction

The coordination chemistry of the group 4 elements Ti, Zr, and Hf has been dominated by complexes containing cyclopentadienyl ligands.[1] The combination of a group 4 metal and two cyclopentadienyl rings, the so-called metallocenes, is of particular current interest because these systems are considered to be the next generation of polymerization catalysts.[2−9] In an effort to expand the coordination chemistry of the group 4 elements we have developed other ancillary ligand environments using the simple strategy of combining different donor types into chelating arrays. Our original ancillary ligand design **I** involved the combination of an amido unit flanked by two phosphine donors in a potentially tridentate chelating array.[10,11] While much new chemistry has accrued with this ligand, the ligand system was prone to phosphine dissociation because of its intrinsic acyclic nature.[12] In an effort to develop similar donor sets and prevent dissociation, we have recently reported[13] the preparation of a macrocyclic version of ligand **I** that is shown as **II** (Chart 1). This macrocycle can be compared to other similar cyclic ligand arrays such as porphyrins, phthalocyanines, tetraazannulenes (TAA), and related systems.[14−18]

One of the attractive features of macrocyclic type ligands is that the cavity size can be such that larger metal ions are forced to sit above the plane of the donors resulting in more exposure of the metal's coordination sphere.[19,20] Such is the case for group 3 and 4 metal complexes incorporating porphyrins and tetraazannulenes.[19−28] However, in some cases it has been

† Professional Officer, UBC Structural Chemistry Laboratory.

(1) Cardin, D. J.; Lappert, M. F.; Raston, C. L. *Chemistry of Organo-Zirconium and -Hafnium Compounds*; Ellis Horwood: West Sussex, U.K., 1986.
(2) Bochmann, M. *J. Chem. Soc., Dalton Trans.* **1996**, 255.
(3) Bochmann, M.; Jaggar, A. J. *J. Organomet. Chem.* **1992**, *424*, C5.
(4) Hlatky, G. G.; Eckman, R. R.; Turner, H. W. *Organomet. Synth.* **1992**, *11*, 1413.
(5) Coughlin, E. B.; Bercaw, J. E. *J. Am. Chem. Soc.* **1992**, *114*, 7606.
(6) Chien, J. C. W.; Tsai, W. M.; Rausch, M. D. *J. Am. Chem. Soc.* **1991**, *113*, 8570.
(7) Kaminsky, W.; Sinn, H. *Transition Metals and Organometallics as Catalysts for Olefin Polymerization*; Springer: New York, 1988.
(8) Hlatky, G. G.; Turner, H. W.; Eckman, R. R. *J. Am. Chem. Soc.* **1989**, *111*, 2728.
(9) Schneider, N.; Huttenloch, M. E.; Stehling, U.; Kirsten, R.; Schaper, F.; Brintzinger, H. H. *Organometallics* **1997**, *16*, 3413.
(10) Fryzuk, M. D. *Can. J. Chem.* **1992**, *70*, 2839.
(11) Fryzuk, M. D.; Berg, D. J.; Haddad, T. S. *Coord. Chem. Rev.* **1990**, *99*, 137.
(12) Fryzuk, M.; Carter, A.; Rettig, S. J. *Organometallics* **1992**, *11*, 469.
(13) Fryzuk, M. D.; Love, J. B.; Rettig, S. J. *J. Chem. Soc., Chem. Commun.* **1996**, 2783.
(14) Buchler, J. W. *The Porphyrins*; Dolphin, D., Ed.; Academic Press, Inc.: New York, 1978; Vol. 1, p 390.
(15) Guillard, R.; Kadish, K. M. *Chem. Rev. (Washington, D.C.)* **1988**, *88*, 1121.
(16) Smith, K. M. *Porpyhrins and Metalloporphyrins*; Elsevier: New York, 1975.
(17) Rogers, A. J.; Solari, E.; Floriani, C.; Chiesi-Villa, A.; Rizzoli, C. *J. Chem. Soc., Dalton Trans.* **1997**, 2385.
(18) Lee, L.; Berg, D. J.; Bushnell, G. W. *Organometallics* **1997**, *16*, 2556.
(19) Brand, H.; Arnold, J. *Coord. Chem. Rev.* **1995**, *140*, 137.
(20) Black, D. G.; Swenson, D. C.; Jordan, R. F.; Rogers, R. D. *Organometallics* **1995**, *14*, 3539.
(21) Brand, H.; Arnold, J. *Organometallics* **1993**, *12*, 3655.
(22) Brand, H.; Capriotti, J. A.; Arnold, J. *Organometallics* **1994**, *13*, 4469.
(23) Brand, H.; Arnold, J. *Angew. Chem., Int. Ed. Engl.* **1994**, *33*, 95.
(24) Floriani, C.; Ciurli, S.; Chiesi-Villa, A.; Guastini, C. *Angew. Chem., Int. Ed. Engl.* **1987**, *26*, 70.
(25) Giannini, L.; Solari, E.; Floriani, C.; Chiesi-Villa, A.; Rizzoli, C. *Angew. Chem., Int. Ed. Engl.* **1994**, *33*, 2204.
(26) Giannini, L.; Solari, E.; Angelis, S. D.; Ward, T. R.; Floriani, C.; Chiesi-Villa, A.; Rizzoli, C. *J. Am. Chem. Soc.* **1995**, *117*, 5801.

S0276-7333(97)00798-X CCC: $15.00
Publication on Web 02/11/1998

Chart 1

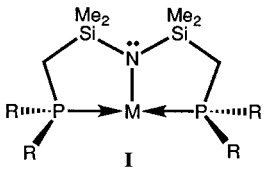

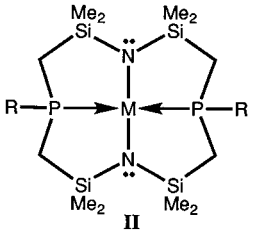

observed that hydrocarbyl ligands show a propensity to migrate from the metal to the imine carbons of such types of macrocycles, thus complicating their usefulness as spectator ligands. In contrast, group 4 complexes incorporating a tetraazamacrocyclic tropocoronand ligand have been shown to be robust against this type of transformation and have shown "metallocene-like" reactivity.[29] In addition, employment of the porphyrinogen skeleton with group 4 metals has yielded complexes that act as carriers for polar organometallics.[30,31] Recently, macrocyclic systems that contain dialkylamido units have been examined as ancillary ligands with Zr(IV).[17,18]

We have recently reported the coordination chemistry of the macrocyclic ligand **II** with zirconium to generate a reactive zirconium dinitrogen species.[32] In this article we report the full details of the syntheses and structures of a variety of organozirconium complexes incorporating this ligand.

Results and Discussion

The high-yield synthesis of the precursor zirconium dichloride complex **1** was accomplished by the reaction of solvated *syn*-$Li_2(S)[P_2N_2]$ (S = THF or dioxane)[13] with $ZrCl_4(THT)_2$ or $ZrCl_4(THF)_2$ as detailed in Scheme 1. The route involving $Li_2(dioxane)[P_2N_2]$ is aided if the dioxane is displaced in-situ, conveniently achieved by conducting the reaction in THF; the product **1** is isolated base free as shown by NMR spectroscopy and elemental analyses.

Crystals of **1** suitable for X-ray diffraction were grown from a saturated toluene solution; the solid-state molecular structure is shown in Figure 1; crystal data are given in Table 1, and selected bond lengths and angles, detailed in Table 2. The complex is observed to adopt a distorted octahedral geometry, with N(1), N(2), Cl(1), and Cl(2) occupying a square plane displaying a combined equatorial angle of 360.4° and P(1) and P(2) in axial positions but pinched back from the optimum 180° to give a P(1)−Zr−P(2) angle of 152.51(6)°, presumably due to the constraints of the macrocyclic framework. The Zr−N, −P, and −Cl bond lengths are not unusual and compare to other Zr−amido and phosphine complexes.[11,12,20,21,32,33]

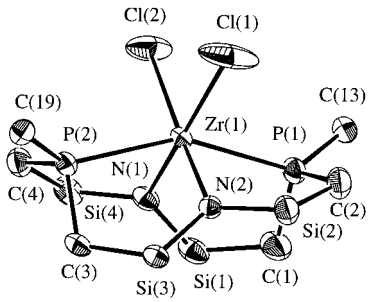

Figure 1. Molecular structure and numbering scheme for $ZrCl_2[P_2N_2]$ (**1**). The silylmethyl substituents have been omitted for clarity as have the phenyl rings attached to phosphorus except that the ipso carbons (C(13) and C(19)) have been retained.

Scheme 1

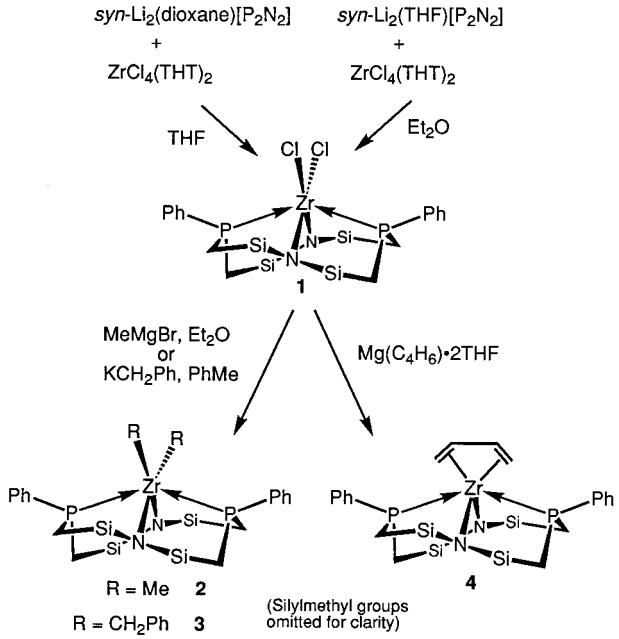

As with zirconium porphyrin and tetraazaannulene (TAA) complexes, the zirconium ion is too large to fit in the 12-membered macrocyclic cavity and thus sits atop the ring skeleton, forcing the remaining chloride ligands to be cis to each other. In porphyrins and related TAA complexes, the distance that the metal is displaced from the plane of the conjugated N_4 plane can be determined; however, it is not possible to easily quantify this effect in the $Zr[P_2N_2]$ complexes reported here since a plane for the nonconjugated P and N donors cannot easily be described. In addition, the P_2N_2 framework is very distorted, adopting a C_2-twist in the solid state which is presumably caused by the trigonal planarity of the $Me_2Si-N-SiMe_2$ links, a feature observed in many metal complexes that incorporate the acyclic $N(SiMe_2CH_2PR_2)_2$ ligand (**I**).

The solid-state structure of **1** (approximate C_2 symmetry) is not reflected in solution at ambient temperature by NMR spectroscopy; the solution structure is more consistent with a C_{2v} symmetry for the ligand substituents. Thus, only two types of silyl methyl

(27) Schaverien, C. J. *J. Chem. Soc., Chem. Commun.* **1991**, 458.
(28) Schaverien, C. J.; Orpen, A. G. *Inorg. Chem.* **1991**, *30*, 4968.
(29) Scott, M. J.; Lippard, S. J. *J. Am. Chem. Soc.* **1997**, *119*, 3411.
(30) Jacoby, D.; Isoz, S.; Floriani, C.; Chiesi-Villa, A.; Rizzoli, C. *J. Am. Chem. Soc.* **1995**, *117*, 2793.
(31) Jacoby, D.; Isoz, S.; Floriani, C.; Schenk, K.; Chiesi-Villa, A.; Rizzoli, C. *Organometallics* **1995**, *14*, 4816.
(32) Fryzuk, M. D.; Love, J. B.; Rettig, S. J.; Young, V. G., Jr. *Science* **1997**, *275*, 1445.

Table 1. Crystallographic Data

compd	**1**[a]	**3**[a]	**4**[a]	**6**[b]
formula	$C_{24}H_{42}Cl_2N_2P_2Si_4Zr$	$C_{38}H_{56}N_2P_2Si_4Zr$	$C_{28}H_{48}N_2P_2Si_4Zr$	$C_{28}H_{51}N_3P_2Si_4Zr$
fw	695.02	806.38	678.21	695.24
color, habit	colorless, prism	yellow, prism	red, irregular	yellow, prism
cryst size, mm	0.30 × 0.45 × 0.45	0.35 × 0.50 × 0.50	0.25 × 0.25 × 0.50	0.20 × 0.35 × 0.40
cryst system	orthorhombic	monoclinic	monoclinic	monoclinic
space group	$P2_12_12_1$ (No. 19)	$C2/c$ (No. 15)	$P2_1/n$ (No. 14)	$P2_1/n$ (No. 14)
a, Å	16.791(1)	28.911(5)	14.378(2)	11.6869(12)
b, Å	21.600(2)	28.921(5)	12.315(2)	21.985(2)
c, Å	9.368(3)	23.112(4)	20.083(3)	14.9311(3)
b, deg	90	108.57(1)	102.76(1)	99.6680(10)
V, Å^3	3397.5(10)	18318(4)	3468.2(9)	3781.9(4)
Z	4	16	4	4
ρ_{calc}, g/cm^3	1.359	1.169	1.299	1.221
F(000)	1440	6784	1424	1464
μ(Mo Kα), cm^{-1}	7.25	4.40	5.67	5.22
transm factors	0.90−1.00	0.87−1.00	0.96−1.00	0.61−1.09[c]
scan type	$\omega-2\theta$	$\omega-2\theta$	$\omega-2\theta$	ω
scan range, deg in ω	0.94 + 0.35 tan θ	1.05 + 0.35 tan θ	1.21 + 0.35 tan θ	0.5
scan rate, deg/min	16 (up to 9 scans)	16 (up to 9 scans)	8 (up to 9 scans)	
data collcd	$+h,+k,+l$	$+h,+k,\pm l$	$+h,+k,\pm l$	full sphere
$2\theta_{max}$, deg	60	50	55	55.8
cryst decay, %	negligible	1.8	4.4	negligible
tot. no. of reflcns	5511	16 868	8667	37 009
no. of unique reflcns	5511	16 469	8344	8946
R_{merge}		0.052	0.038	0.055
reflcns with $I \geq 3\sigma(I)$	2980	6262	4010	4934
no. of variables	317	848	334	343
$R(F, I \geq 3\sigma(I))$	0.039	0.046	0.034	0.041
$R_w(F, I \geq 3\sigma(I))$	0.033	0.045	0.031	0.025
$R(F^2$, all data)				0.066
$R_w(F^2$, all data)				0.053
gof	1.69	2.04	1.57	1.83
max Δ/σ (final cycle)	0.0007	0.001	0.001	0.001
residual density, e/Å^3	−0.71 to +0.80	−0.34 to +0.49	−0.30 to +0.40	−1.19 to +1.24

[a] Temperature 294 K, Rigaku AFC6S diffractometer, Mo $K\alpha$ radiation (λ = 0.710 69 Å), graphite monochromator, takeoff angle 6.0°, aperture 6.0 × 6.0 mm at a distance of 285 mm from the crystal, stationary background counts at each end of the scan (scan/background time ratio 2:1, up to 8 rescans), $\sigma^2(F^2) = [S^2(C + 4B)]/Lp^2$ (S = scan rate, C = scan count, B = normalized background count), function minimized $\sum w(|F_o| - |F_c|)^2$, where $w = 4F_o^2/\sigma^2(F_o^2)$, $R = \sum||F_o| - |F_c||/\sum|F_o|$, $R_w = (\sum w(|F_o| - |F_c|)^2/\sum w|F_o|^2)^{1/2}$, and gof = $[\sum w(|F_o| - |F_c|)^2/(m - n)]^{1/2}$. Values given for R, R_w, and gof are based on those reflections with $I \geq 3\sigma(I)$. [b] Temperature 294 K, Rigaku/ADSC CCD diffractometer, Mo $K\alpha$ radiation (λ = 0.710 69 Å), graphite monochromator, takeoff angle 6.0°, aperture 94 × 94 mm at a distance of 39.116(5) mm from the crystal, 460 frames at 60 s/image, function minimized $\sum w(|F_o^2| - |F_c^2|)^2$, with $w = 1/[3(\sigma(F_o^2) + 0.01(F_o^2))]$, where $\sigma(F_o^2)$ is based on counting statistics, $R = \sum||F_o^2| - |F_c^2||/\sum|F_o^2|$, $R_w = (\sum w(|F_o^2| - |F_c^2|)^2/\sum w|F_o^2|^2)^{1/2}$, and gof = $[\sum w(|F_o^2| - |F_c^2|)^2/(m - n)]^{1/2}$. Values given for R, R_w, and gof are based on all reflections. [c] Includes corrections for decay and absorption.

Table 2. Selected Bond Lengths (Å) and Angles (deg) in $ZrCl_2[P_2N_2]$ (1)

Zr(1)−N(1)	2.136(4)	Zr(1)−N(2)	2.125(4)
Zr(1)−P(1)	2.694(2)	Zr(1)−P(2)	2.707(2)
Zr(1)−Cl(1)	2.455(2)	Zr(1)−Cl(2)	2.448(2)
N(1)−Zr(1)−N(2)	96.8(2)	P(1)−Zr(1)−P(2)	152.52(6)
Cl(1)−Zr(1)−Cl(2)	82.57(7)	N(1)−Zr(1)−Cl(2)	89.5(1)
N(2)−Zr(1)−Cl(1)	91.3(1)		

protons are observed in the ^{1}H NMR spectrum at 0.34 and 0.30 ppm for 12H each, reflecting "top and bottom" asymmetry of **1**. The *o*-protons of the phosphine phenyl rings are distinct as a multiplet at 7.84 ppm; the CH_2 protons of the ring appear as AB multiplets coupled to phosphorus centered at 1.30 ppm. The phosphorus nuclei are equivalent, with a singlet at −14.3 ppm observed in the $^{31}P\{^1H\}$ spectrum. It is therefore apparent that the $[P_2N_2]$ macrocyclic framework is quite flexible in solution and undergoes dynamic processes which can be visualized as a "rocking" motion centered at the trigonal silylamide groups. The chemical shifts and coupling patterns observed in the ^{1}H NMR spectrum appear to be diagnostic for the $[P_2N_2]$ ligand coordinated to a large metal (see later).

The reaction between the dichloride **1** and typical alkylating agents was found to yield the desired dialkylzirconium complexes in high yield (see Scheme 1), although the choice of alkylating agent appears critical. Thus, while the reaction between **1** and MeMgBr in Et_2O produces colorless $ZrMe_2[P_2N_2]$ (**2**) in 85% yield, the analogous reaction using MeLi produces a dark brown material from which only low yields of **2** (<5%) can be isolated. The rapid reaction between **1** and KCH_2Ph in toluene is simpler, resulting in good yields of the orange dibenzyl complex $Zr(CH_2Ph)_2[P_2N_2]$ (**3**). This latter complex appears to be sensitive to decomposition in solution; a sample of **3** in toluene-d_8 decomposes to a number of unidentified complexes over a period of 48 h. Also, even in the absence of air and moisture, the dimethyl complex undergoes decomposition to a complex number of products in the solid state over a period of 24 h.

In a manner similar to the dichloride **1**, both dialkyls adopt C_{2v}-symmetric structures in solution at ambient temperatures as evidenced by NMR spectroscopy, and therefore a cis-orientation of the alkyl ligands is a reasonable conclusion. In **2**, the methyl protons are observed as a triplet coupled to phosphorus at 1.07 ppm (J_{PH} 4.7 Hz) and overlap with the resonances due to the ring CH_2 protons. Likewise in **3**, the methylene protons of the benzyl groups are observed as a triplet at 2.16 ppm (J_{PH} 3.0 Hz). Both complexes exhibit singlet resonances in their respective $^{31}P\{^1H\}$ NMR spectra.

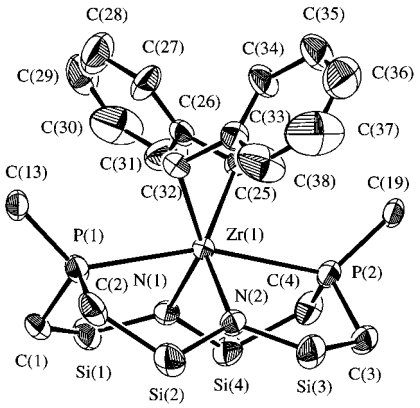

Figure 2. Molecular structure and numbering scheme for $Zr(CH_2Ph)_2[P_2N_2]$ (**3**). The silylmethyl substituents have been omitted for clarity as have the phenyl rings attached to phosphorus except that the ipso carbons (C(13) and C(19)) have been retained.

Table 3. Selected Bond Lengths (Å) and Angles (deg) in $Zr(CH_2Ph)_2[P_2N_2]$ (3)

Zr(1)−N(1)	2.170(6)	Zr(1)−N(2)	2.192(6)
Zr(1)−P(1)	2.730(2)	Zr(1)−P(2)	2.715(2)
Zr(1)−C(25)	2.345(8)	Zr(1)−C(32)	2.335(8)
N(1)−Zr(1)−N(2)	98.0(2)	P(1)−Zr(1)−P(2)	159.73(8)
C(25)−Zr(1)−C(32)	85.0(3)	N(1)−Zr(1)−C(25)	97.4(3)
N(2)−Zr(1)−C(32)	98.7(3)	Zr(1)−C(25)−C(26)	112.6(5)
Zr(1)−C(32)−C(33)	112.9(6)		

The dibenzyl complex **3** was crystallized as orange prisms from a cooled mixture of toluene and hexanes; the solid-state structure is shown in Figure 2, with crystal data and selected bond lengths and angles detailed in Tables 1 and 3, respectively. The substitution of the chloride ligands in **1** for the benzyl ligands in **3** has resulted in some structural changes to the macrocyclic framework, with increases in both the phosphine and amide "bite angles", P(1)−Zr−P(2) and N(1)−Zr−N(2): 152.51(6) and 96.8(2)°, respectively, in **1** to 159.73(8) and 98.0(2)° in **3**. Unlike **1**, the ligand arrangement around the zirconium center in **3** is best described as trigonal antiprismatic with the two trigonal planes described by N(1)P(2)C(25) and N(2)P(1)C(32); the methylene carbons C(25) and C(32) of the benzyl groups are not located in a square plane involving the two amido nitrogens but are instead rotated considerably out of this plane. This feature may in part be due to steric interactions between the benzylic and macrocyclic phenyl groups. The benzyl groups are observed to be coordinated in an η^1-manner, with the zirconium−carbon bond lengths of 2.335(8) and 2.345(8) Å comparable to those observed in other zirconium alkyl complexes incorporating amido ligands; the $Zr-CH_2-C_{ipso}$ angles are also relatively obtuse at 112.9(6) and 112.6(5)°.[20,24,26] The lack of any η^2-character in the benzyl ligands[34,35] suggests that the zirconium center supported by the $[P_2N_2]$ ligand is not particularly electrophilic perhaps due to the presence of the soft phosphine donors.

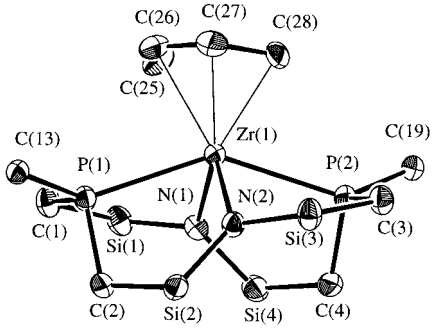

Figure 3. Molecular structure and numbering scheme for $Zr(\eta^4\text{-}C_4H_6)[P_2N_2]$ (**4**). The silylmethyl substituents have been omitted for clarity as have the phenyl rings attached to phosphorus except that the ipso carbons (C(13) and C(19)) have been retained.

Table 4. Selected Bond Lengths (Å) and Angles (deg) in $Zr(\eta^4\text{-}C_4H_6)[P_2N_2]$ (4)

Zr(1)−N(1)	2.217(3)	Zr(1)−N(2)	2.189(3)
Zr(1)−P(1)	2.707(1)	Zr(1)−P(2)	2.701(1)
Zr(1)−C(25)	2.416(4)	Zr(1)−C(26)	2.445(4)
Zr(1)−C(27)	2.445(4)	Zr(1)−C(28)	2.380(4)
C(25)−C(26)	1.379(6)	C(26)−C(27)	1.408(6)
C(27)−C(28)	1.400(6)		
N(1)−Zr(1)−N(2)	101.4(1)	P(1)−Zr(1)−P(2)	143.53(3)
Zr(1)−C(25)−C(26)	74.7(3)	Zr(1)−C(28)−C(27)	75.7(2)

The isolation of the dimeric zirconium dinitrogen complex $\{[P_2N_2]Zr\}_2(\mu\text{-}N_2)$, formed by reduction of the dichloride **1** under N_2,[32] suggested that diene complexes incorporating the $Zr[P_2N_2]$ fragment could be accessed.[36] Cyclopentadienyl-based zirconium butadiene complexes activated by $B(C_6F_5)_3$ have also shown promise as methylaluminoxane-free Ziegler-type catalysts.[37] The reaction between **1** and $Mg(C_4H_6)\cdot 2THF$ in THF resulted in the formation of the deep red butadiene complex $Zr(\eta^4\text{-}C_4H_6)[P_2N_2]$ (**4**) in moderate yield (Scheme 1). Crystals suitable for X-ray crystallography were grown from hexanes; the molecular structure is shown in Figure 3, with crystal data and selected bond lengths and angles detailed in Tables 1 and 4, respectively. Analysis of the butadiene C−C and Zr−C bond lengths suggests that this interaction is best described in terms of a π:η^4-coordination mode rather than σ^2:π; the internal butadiene carbons are slightly closer to the zirconium center than the terminal carbons [Zr(1)−C(26)/C(27) = 2.445 (4) Å; Zr(1)−C(25)/C(28) = 2.416(4) and 2.380(4) Å] coupled with the observation that the C−C bonds do not alternate in the long−short−long manner expected for σ^2:π bonding.[38] A better gauge of the bonding mode of the butadiene fragment is to compare bond lengths M−C(2) and C(1)−C(2) and the bond angle M−C(1)−C(2); higher values should be evident for a σ^2:π interaction.[39,40] In the case of **4**, the values of 2.445(4) and 1.379(6) Å and 74.7(3)° for Zr(1)−C(26), C(25)−C(26), and Zr(1)−C(25)−C(26), re-

(33) Angelis, S. D.; Solari, E.; Gallo, E.; Floriani, C.; Chiesi-Villa, A.; Rizzoli, C. *Inorg. Chem.* **1992**, *31*, 1.
(34) Latesky, S. L.; McMullen, A. K.; Niccolai, G. P.; Rothwell, I. P.; Huffman, J. C. *Organometallics* **1985**, *4*, 902.
(35) Cloke, F. G. N.; Geldbach, T. J.; Hitchcock, P. B.; Love, J. B. *J. Organomet. Chem.* **1996**, *506*, 343.
(36) Fryzuk, M. D.; Haddad, T. S.; Rettig, S. J. *J. Am. Chem. Soc.* **1990**, *112*, 8185.
(37) Temme, B.; Erker, G.; Karl, J.; Luftmann, H.; Frohlich, R.; Kotila, S. *Angew. Chem., Int. Ed. Engl.* **1995**, *34*, 1775.
(38) Diamond, G. M.; Green, M. L. H.; Walker, N. M.; Howard, J. A. K.; Mason, S. A. *J. Chem. Soc., Dalton Trans.* **1992**, 2641.
(39) Kruger, C.; Muller, G.; Erker, G.; Dorf, U.; Engel, K. *Organometallics* **1985**, *4*, 215.
(40) Erker, G.; Engel, K.; Kruger, C.; Muller, G. *Organometallics* **1984**, *3*, 128.

spectively, compare well with those reported for π:η^4-butadiene complexes containing amido-, chloride-, or alkoxy-based ligands.[25,38,41,42] More general comparisons have also been made across the periodic table using the empirical relationship that exists between the butadiene dihedral angle ϕ and $\Delta\delta$, the difference between the distances of the internal and external carbons to the metal [average($Zr-C_{ter}$) − average($Zr-C_{int}$) = 2.398 − 2.445 = −0.047 Å].[43] Again, the low value of $\Delta\delta$ (−0.047) and the ϕ value of 85.2 are diagnostic of π:η^4-bonding.[41]

In a manner similar to the dichloride **1** and the dibenzyl **3**, the backbone of the [P_2N_2] ligand in **4** shows a C_2-twist in the solid state. In this case, the N(1)−Zr-(1)−N(2) and P(1)−Zr(1)−P(2) bite angles are 101.4(1) and 143.53(3)°, respectively, which are similar to those observed for **3** and **4**; similar Zr−N and Zr−P bond lengths are also observed.

The solution structure reflects that observed in the solid state. Inspection of the $^{31}P\{^1H\}$ NMR spectrum reveals a second-order AB pattern for nonequivalent phosphorus nuclei centered at −6.1 ppm with a large PP coupling of 78.1 Hz. This asymmetry is mirrored in the ^1H NMR spectrum, in which broad features attributable to the silyl methyl protons are observed, along with broad signals due to the *o*-protons of the phenyl rings. On cooling of a sample of **4** in C_7D_8, these resonances sharpen at 270 K, resulting in four silyl methyl resonances and two *o*-proton signals, consistent with a macrocyclic framework in which the phosphorus donors are nonequivalent with a mirror plane bisecting the N(1)−Zr(1)−N(2) angle, thus requiring that the butadiene fragment is also bisected at the C(26)−C(27) bond by this plane; this is shown as **4′** in Figure 4.

No change in these resonances was observed upon further cooling to 215 K. The broad multiplets displayed at δ 5.78 (2H), 2.23 (2H), and 0.80 ppm (2H), for the meso-, syn-, and anti-butadiene protons, respectively, also sharpen upon cooling although the expected low-temperature limiting spectrum of C_1 symmetry found in the solid state was not obtained. The dynamic processes occurring in solution for **4** are commensurate with the butadiene unit undergoing a restricted rotation or rocking motion, as full rotation or envelope flipping processes would equilibrate the phosphine donors and in the latter case would also exchange the syn- and anti-butadiene protons, neither of which are observed here.[38,41]

Mononuclear imido complexes of the group 4 metals have been found to display unique reactivity, for example undergoing a range of cycloaddition reactions and participating in the activation of sp^2 and sp^3 C−H bonds.[44−47] Recently, the synthesis and reactivity of group 4 imido complexes incorporating tetraazaannulene ligands were reported.[48,49]

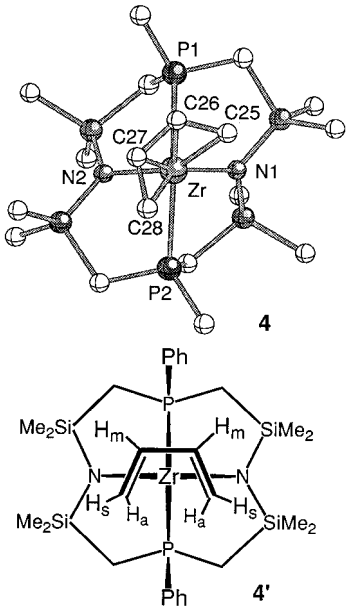

Figure 4. Top: Model (ball and stick) showing the solid-state structure of Zr(η^4-C_4H_6)[P_2N_2] (**4**) looking down the Zr−centroid axis. Bottom: Schematic showing the average structure in solution having C_s symmetry.

Scheme 2

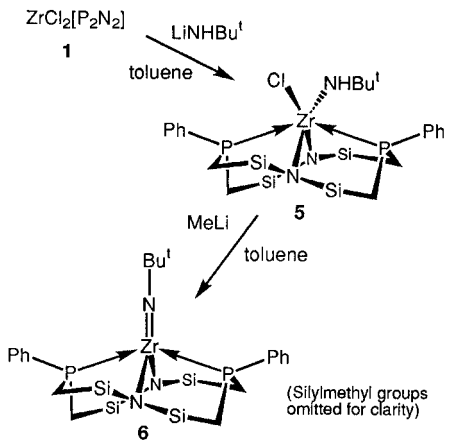

The synthesis of the imido complex Zr(NBu^t)[P_2N_2] (**6**) was successfully achieved by following procedures developed for the generation of the transient zirconocene imido complex $Cp_2Zr{=}NBu^t$ (see Scheme 2).[46]

The reaction between **1** and 1 equiv of $LiNHBu^t$ in Et_2O led to the formation of a compound that we presume is the amido−chloride complex ZrCl($NHBu^t$)-[P_2N_2] (**5**). Satisfactory microanalytical data were not obtained due to the high solubility of **5** in aliphatic hydrocarbons, although ^1H and $^{31}P\{^1H\}$ NMR data indicated ca. 95% purity. The ^1H NMR spectrum shows the presence of one $NHBu^t$ group per [P_2N_2] macrocycle, with resonances due to the NH and Bu^t groups observed at δ 7.33 and 1.38 ppm, respectively; curiously, the silylmethyl protons on the ring give rise to a broad singlet. The $^{31}P\{^1H\}$ NMR data, a singlet at δ −16.7 ppm, coupled with the above ^1H NMR data suggest that

(41) Fryzuk, M. D.; Haddad, T. S.; Rettig, S. J. *Organometallics* **1989**, *8*, 1723.
(42) Giannini, L.; Solari, E.; Zanotti-Gerosa, A.; Floriani, C.; Chiesi-Villa, A.; Rizzoli, C. *Angew. Chem., Int. Ed. Engl.* **1996**, *35*, 85.
(43) Yasuda, H.; Nakamura, A.; Kai, Y.; Kasai, N. *Topics in Physical Organometallic Chemistry*; Freund Publishing House: Tel Aviv, 1987; Vol. 2.
(44) Lee, S. Y.; Bergman, R. G. *J. Am. Chem. Soc.* **1995**, *117*, 5877.
(45) Walsh, P. J.; Baranger, A. M.; Bergman, R. G. *J. Am. Chem. Soc.* **1992**, *114*, 1708.
(46) Walsh, P. J.; Hollander, F. J.; Bergman, R. G. *Organometallics* **1993**, *12*, 3705.
(47) Schaller, C. P.; Cummins, C. C.; Wolczanski, P. T. *J. Am. Chem. Soc.* **1996**, *118*, 591.
(48) Nikonov, G. I.; Blake, A. J.; Mountford, P. *Inorg. Chem.* **1997**, *36*, 1107.
(49) Blake, A. J.; Mountford, P.; Nikonov, G. I.; Swallow, D. *J. Chem. Soc., Chem. Commun.* **1996**, 1835.

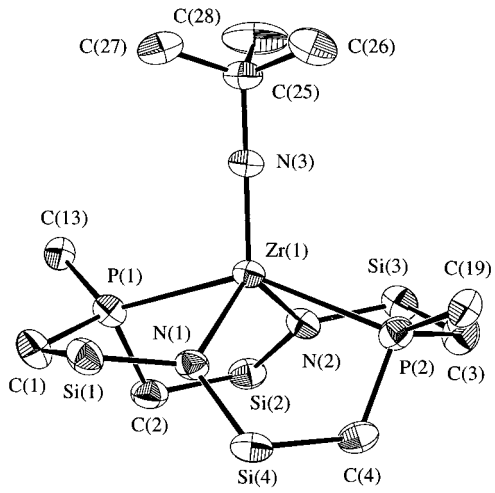

Figure 5. Molecular structure and numbering scheme for $Zr(NBu^t)[P_2N_2]$ (**6**). The silylmethyl substituents have been omitted for clarity as have the phenyl rings attached to phosphorus except that the ipso carbons (C(13) and C(19)) have been retained.

Table 5. Selected Bond Lengths (Å) and Angles (deg) in $Zr(NBu^t)[P_2N_2]$ (6)

Zr(1)−N(1)	2.210(2)	Zr(1)−N(2)	2.203(2)
Zr(1)−P(1)	2.7114(7)	Zr(1)−P(2)	2.7360(7)
Zr(1)−N(3)	1.8413(15)	N(3)−C(25)	1.457(2)
N(1)−Zr(1)−N(2)	115.55(6)	P(1)−Zr(1)−P(2)	145.54(2)
N(1)−Zr(1)−N(3)	123.59(7)	N(2)−Zr(1)−N(3)	120.82(7)
P(1)−Zr(1)−N(3)	105.60(5)	P(2)−Zr(1)−N(3)	108.85(5)
Zr(1)−N(3)−C(25)	179.50(15)		

this complex is fluxional; this behavior was not investigated further.

The reaction between crude **5** and 1 equiv of MeLi in Et_2O at −78 °C led to the direct formation of the imido complex $Zr(NBu^t)[P_2N_2]$ (**6**) in high yield as evidenced by ^1H NMR spectroscopy; however, the isolated yield was low due to the high solubility of this complex in aliphatic hydrocarbons.

The ^1H NMR spectrum of **6** in C_6D_6 concurs with a C_{2v}-symmetric solution structure, displaying two resonances for the ring silylmethyl protons and a singlet for the imido Bu^t group. Also, the $^{31}P\{^1H\}$ NMR spectrum is a singlet at −15.5 ppm.

Complex **6** crystallized from hexanes at −40 °C as orange blocks that were suitable for X-ray crystallography. The solid-state structure of **6** is shown in Figure 5, with crystal data and selected bond lengths and angles detailed in Tables 1 and 5, respectively. It is immediately evident that **6** is monomeric in the solid state, with the geometry at the zirconium best described as distorted trigonal bipyramidal; N(1), N(2), and N(3) are in the trigonal plane [N(1)−Zr(1)−N(2) 115.55(6)°, N(1)−Zr(1)−N(3) 123.59(7)°, N(2)−Zr(1)−N(3) 120.82(7)°], and P(1) and P(2) are apical, albeit pinched back [P(1)−Zr(1)−P(2) = 145.54(2)°] in a manner similar to that described above. From this structure and those described above, it is apparent that the $[P_2N_2]$ macrocycle is able to adopt a range of geometries when coordinated to a metal, from pseudo-octahedral (N−Zr−N = 96.8−101.4°) to distorted trigonal planar (N−Zr−N = 115.6°) and that this effect is largely metal induced. The phosphine "bite-angle" also covers a large range (143.5−159.7°). The Zr−N(amido) and Zr−P bond lengths are similar to those observed in **1**, **3**, and **4**. The Bu^t-imido unit is almost perfectly linear with a Zr(1)−N(3)−C(25) angle of 179.50(15)°; a correspondingly short Zr(1)−N(3) bond length of 1.8413(15) Å is also observed. These values are comparable to those reported in the limited number of structurally characterized zirconium imido complexes, in which the Zr═N bond length ranges from 1.826(4) to 1.876(4) Å and the Zr−N−C bond angle from 164.5(3) to 175.5(8)° (not including silyl[47] or phosphaalkenyl[50] substituted imides which fall outside these ranges).[46,51−54] A detailed structural and theoretical analysis of five-coordinate zirconium imido complexes has been reported;[52] this concluded that while complexes of the type $Zr(NAr)(NAr_2)_2(py')_2$ contain amido ligands that are capable of a π-interaction with the d_{xy} orbitals on the zirconium center (z-direction along the Zr═N vector), such an overlap does not interfere with the overlaps between the zirconium d_{xz} and d_{yz} orbitals and the p_x and p_y sp-hybridized orbitals of the imido nitrogen that form the $Zr-N_{imido}$ triple bond, although the former interaction does result in a lengthening of the $Zr-N_{amido}$ bond. In the case of **6**, the linearity of the Zr−N−C bond angle suggests that the interaction between the zirconium and imido nitrogen is also best viewed as a triple bond, in common with those previously reported, although in this case it is difficult to discern whether significant lengthening of the $Zr-N_{amido}$ bond distances of the macrocycle has occurred, since the π-electron density could be delocalized over the Si−N−Si unit; $Zr-N_{amido}$ bond distances for the $Zr[P_2N_2]$ fragment range from 2.125(4) to 2.254(3) Å.

As described above, the transient, base-free, monomeric zirconium imido complexes $Cp_2Zr{=}NBu^t$ and $(Bu^t{}_3SiNH)_2Zr{=}NSiBu^t{}_3$, formed in-situ by heating the appropriate alkylamido complex, are able to activate sp^2 and sp^3 C−H bonds, respectively. In the formation of **6**, however, there was no evidence that the putative alkylamido intermediate $Zr(NHBu^t)Me[P_2N_2]$ was stable with respect to alkane elimination, with the imido complex **6** being formed directly; **6** was found to be unreactive toward aromatic C−H bonds and also toward H_2.

Conclusions

In this work, we have provided full details of the preparation and structures of a series of Zr(IV) complexes that incorporate the macrocyclic bis(amido−phosphine) ligand $[P_2N_2]$. The dichloride complex $ZrCl_2[P_2N_2]$ serves as a useful entry into bis(hydrocarbyl) derivatives, $ZrR_2[P_2N_2]$, by metathesis type procedures, although some care must be exercised as to the alkylating agent used. The butadiene complex $Zr(\eta^4\text{-}C_4H_6)[P_2N_2]$ has been prepared and structurally characterized; on the basis of the solid-state molecular structure, the $\pi{:}\eta^4$ description of the bonding seems more apt that the $\sigma^2{:}\pi$ formalism. Finally, we also have included the

(50) Breen, T. L.; Stephan, D. W. *J. Am. Chem. Soc.* **1995**, *117*, 11914.
(51) Profilet, R. D.; Zambrano, C. H.; Fanwick, P. E.; Nash, J. J.; Rothwell, I. P. *Inorg. Chem.* **1990**, *29*, 4362.
(52) Zambrano, C. S.; Profilet, R. D.; Hill, J. E.; Fanwick, P. E.; Rothwell, I. P. *Polyhedron* **1993**, *12*, 689.
(53) Bai, Y.; Roesky, H. W.; Noltemeyer, M.; Witt, M. *Chem. Ber.* **1992**, *125*, 825.
(54) Arney, D. J.; Bruck, M. A.; Huber, S. R.; Wigley, D. E. *Inorg. Chem.* **1992**, *31*, 3749.

imido complex $Zr(NBu^t)[P_2N_2]$ which shows a completely linear Zr−N−C unit. The imide unit does not undergo C−H activation processes.

All of the solid-state molecular structures reported here show that the macrocyclic ligand, upon coordination to Zr(IV), distorts to generate a pseudo-C_2-symmetric arrangement of the $Zr[P_2N_2]$ unit. However, in solution, the flexibility of the macrocycle allows conformational motion that symmetrizes the $Zr[P_2N_2]$ portion of the system.

Experimental Section

Unless otherwise stated all manipulations were performed under an atmosphere of dry, oxygen-free dinitrogen or argon by means of standard Schlenk or glovebox techniques (Vacuum Atmospheres HE-553-2 glovebox equipped with a MO-40-2H purification system and a −40 °C freezer). Diethyl ether, hexanes, and tetrahydrofuran (sodium benzophenone ketyl) and toluene (sodium) were dried and distilled prior to use. Argon was dried and deoxygenated by passing the gases through a column containing molecular sieves and MnO. Deuterated tetrahydrofuran and benzene were refluxed over potassium metal under partial pressure, trap-to-trap distilled, and freeze−pump−thaw degassed three times. Deuterated toluene was distilled from sodium benzophenone ketyl and freeze−pump−thaw degassed three times. Unless otherwise stated, ^1H and $^{31}P\{^1H\}$ NMR spectra were recorded on a Bruker AC-200 instrument operating at 200 and 81.0 MHz, respectively, and $^1H\{^{31}P\}$ NMR spectra were recorded on a Bruker AMX-500 instrument operating at 500.1 MHz. Variable-temperature NMR spectra were recorded on Varian XL300 and Bruker AMX-500 instruments. ^1H NMR spectra were referenced to internal C_6D_5H (7.15 ppm), C_7D_7H (2.09 ppm), and C_4D_7HO (3.58 ppm), and $^{31}P\{^1H\}$ NMR spectra to external $P(OMe)_3$ (141.0 ppm with respect to 85% H_3PO_4 at 0.0 ppm).

The compounds $Li_2(THF)[P_2N_2]$, $Li_2(dioxane)[P_2N_2]$,[13] $ZrCl_4(THT)_2$ (THT = tetrahydrothiophene),[21] KCH_2Ph, and $[Mg(THF)_2(C_4H_6)]_n$ were prepared according to literature procedures. $LiNHBu^t$ was prepared by treating a solution of NH_2Bu^t in Et_2O with 1 molar equiv of $LiBu^n$ and evaporating to dryness. The 3.0 M MeMgBr in Et_2O was purchased from Aldrich.

Microanalyses (C, H, N) were performed by Mr. P. Borda of this department.

Preparation of $ZrCl_2[P_2N_2]$ (1). Method 1. To a stirred mixture of $Li_2(THF)[P_2N_2]$ (1.35 g, 2.13 mmol) and $ZrCl_4(THT)_2$ (0.96 g, 2.34 mmol) was added Et_2O (30 mL) at −20 °C. Upon warming of the sample to room temperature, the solids began to dissolve and a fresh, white precipitate was observed. The mixture was then stirred at this temperature for 16 h, after which the solvents were evaporated in vacuo, the off-white residue was extracted into toluene (2 × 15 mL), and the mixture was filtered through Celite. Partial evaporation of the filtrate and cooling to −30 °C caused the deposition of **1** as pale yellow plates. Yield: 1.25 g, 85%.

Method 2. To a stirred mixture of $Li_2(dioxane)[P_2N_2]$ (0.58 g, 0.91 mmol) and $ZrCl_4(THT)_2$ (0.37 g, 0.91 mmol) was added THF (10 mL) at −78 °C. Upon warming of the sample to room temperature, the solids dissolved; the resultant pale yellow solution was stirred at this temperature for 30 min and then evaporated to dryness. The residues were extracted into toluene (2 × 5 mL), the mixture was filtered through Celite, and the filtrate was evaporated to dryness. The filtered residues were washed with hexanes (2 × 2 mL) and dried under vacuum, yielding 0.532 g, 84%, of **1** as an off-white powder. No significant change in chemical yield was observed when $ZrCl_4(THF)_2$ was used in place of $ZrCl_4(THT)_2$.

Anal. Calcd for $C_{24}H_{42}Cl_2N_2P_2Zr$: C, 41.48; H, 6.09; N, 4.03. Found: C, 42.05; H, 6.29; N, 4.08. ^1H NMR (C_6D_6, 500 MHz): δ 7.84 (m, 4H, *o*-H), 7.04 (m, 6H, *m*, *p*-H), 1.37 (ABX m, 4H, CH_2 ring), 1.24 (ABX m, 4H, CH_2 ring), 0.34 (s, 12H, $SiMe_2$ ring), 0.30 (s, 12H, $SiMe_2$ ring). $^{31}P\{^1H\}$: δ −14.3 (s).

Preparation of $ZrMe_2[P_2N_2]$ (2). To a slurry of $ZrCl_2[P_2N_2]$ (0.50 g, 0.72 mmol) in Et_2O (20 mL) was added 3.0 M MeMgBr in Et_2O (0.5 mL, 1.44 mmol) at room temperature; over a period of a few minutes, the solids dissolved and then a colorless precipitate was formed. The slurry was stirred for 1.5 h and evaporated to dryness, the residue was extracted into toluene (2 × 5 mL), and the extract was filtered through Celite. The pale yellow filtrate was evaporated to dryness to yield 0.398 g, 85%, of **2** as an off-white powder. This material is thermally- and photochemically-sensitive; as a result numerous attempts to obtain elemental analyses failed.

^1H NMR (C_6D_6, 500 MHz): δ_H 7.72 (m, 4H, *o*-H phenyl), 7.17 (m, 6H, *m*/*p*-H phenyl), 1.25 (m, 4H, ring CH_2), 1.07 (t + m, 10H, J_{PH} 4.7 Hz, Zr−CH_3 overlapping with ring CH_2), 0.26 (s, 12H, ring $SiMe_2$), 0.25 (s, 12H, ring $SiMe_2$). $^{31}P\{^1H\}$ NMR: δ_P −18.4 (s)

Preparation of $Zr(CH_2Ph)_2[P_2N_2]$ (3). In the glovebox, KCH_2Ph (0.375 g, 2.88 mmol) was added as a solid to a stirred solution of $ZrCl_2[P_2N_2]$ (1.00 g, 1.44 mmol) in toluene (30 mL) at ambient temperature, the red solids slowly dissolving. The mixture was stirred for 1.5 h and filtered through Celite, and the yellow filtrate was evaporated to ca. 2 mL. The addition of hexanes (10 mL) and cooling to −30 °C caused **3** to deposit as orange prisms, yield 0.72 g, 62%.

Anal. Calcd for $C_{38}H_{56}N_2P_2Si_4Zr$: C, 56.60; H, 7.00; N, 3.47. Found: C, 56.83; H, 7.00; N, 3.50. ^1H NMR ($CD_3C_6D_5$, 200 MHz): δ 7.15−6.8 (m's, 20 H, phenyl), 2.16 (t, 4H, J_{PH} = 3.0 Hz, Zr−CH_2Ph), 1.20 (m, 8H, CH_2 ring), 0.42 (s, 12H, $SiMe_2$ ring), 0.35 (s, 12H, $SiMe_2$ ring). $^{31}P\{^1H\}$ δ −7.51 (s).

Preparation of $Zr(\eta^4\text{-}C_4H_6)[P_2N_2]$ (4). THF (10 mL) was added to an intimate mixture of $ZrCl_2[P_2N_2]$ (0.238 g, 0.342 mmol) and $Mg(C_4H_6)_2{\cdot}2THF$ (76 mg, 0.342 mmol) at −78 °C. Upon warming of the sample to room temperature, the solids dissolved, resulting in the formation of a deep red solution which was stirred for 4.5 h, then evaporated to dryness; the residue was extracted into hexanes (2 × 10 mL), and the extract was filtered through Celite. Partial evaporation of the filtrate and cooling to −30 °C yielded 0.135 g, 58%, of **4** as dark red blocks.

Anal. Calcd for $C_{28}H_{48}N_2P_2Si_4Zr$: C, 49.59; H, 7.13; N, 4.13. Found: C, 49.42; H, 7.22; N, 4.00. ^1H NMR (C_6D_6, 500 MHz): δ_H 7.63 (br s, 2H, *o*-H phenyl), 7.56 (br s, 2H, *o*-H phenyl), 7.14 (m, 6H, *m*/*p*-H phenyl), 5.84 (m, 2H, H_{meso}), 2.48 (m, 2H, H_{syn}), 1.37 (m, 4H, ring CH_2), 1.18 (m, 4H, ring CH_2), 0.67 (m, 2H, H_{anti} of C_4H_6), 0.39 (br s, 6H, ring $SiMe_2$), 0.34 (br s, 6H, ring $SiMe_2$), 0.27 (br s, 6H, ring $SiMe_2$), 0.09 (br s, 6H, ring $SiMe_2$). ^1H NMR (C_6D_6, 280 K, 500 MHz): δ_H 7.63 (m, 2H, *o*-H phenyl), 7.53 (m, 2H, *o*-H phenyl), 7.14 (m, 6H, *m*/*p*-H phenyl), 5.89 (m, 2H, H_{meso}), 2.51 (m, 2H, H_{syn}), 1.36 (m, 4H, ring CH_2), 1.14 (m, 4H, ring CH_2), 0.72 (m, 2H, H_{anti} of C_4H_6), 0.43 (s, 6H, ring $SiMe_2$), 0.39 (s, 6H, ring $SiMe_2$), 0.30 (s, 6H, ring $SiMe_2$), 0.12 (s, 6H, ring $SiMe_2$). $^{31}P\{^1H\}$ NMR: δ_P −6.1 (second-order AB doublet with wings, J_{PP} 78.1 Hz).

Preparation of $ZrCl(NHBu^t)[P_2N_2]$ (5). A solution of $LiNHBu^t$ (30 mg, 0.38 mmol) in toluene (2 mL) was added dropwise to a stirred solution of $ZrCl_2[P_2N_2]$ (0.265 g, 0.38 mmol) in toluene (10 mL) at room temperature. The resultant mixture was stirred at this temperature for 2 h, after which it was evaporated to dryness. The residue was extracted into hexanes, and the extract was filtered through Celite. Evaporation of the yellow filtrate yielded an oily solid, 212 mg, 76%. The high solubility of **5** in hydrocarbon solvents precluded the isolation of an analytically pure material, although 95% purity was observed by NMR spectroscopy.

^1H NMR (C_6D_6, 500 MHz): δ_H 7.82 (m, 4H, *o*-H), 7.33 (s, 1H, NH), 7.18 (m, 4H, *m*-H), 7.09 (m, 2H, *p*-H phenyl), 1.38

(s, 17H, C(CH_3)$_3$ + ring CH_2), 0.43 (br s, 12H, ring $SiMe_2$). $^{31}P\{^1H\}$ NMR (C_6D_6): δ_P −16.7 (s).

Preparation of Zr(NBu^t)[P_2N_2] (6). A solution of MeLi (1.6 M, 0.18 mL, 0.29 mmol) in Et_2O was added dropwise to a stirred solution of crude ZrCl(NHBu^t)[P_2N_2] (212 mg, 0.29 mmol) in toluene (10 mL) at room temperature, causing a colorless solid to precipitate. The mixture was stirred at this temperature for 1 h and evaporated to dryness, the solid was extracted into hexanes (2 × 5 mL), and the extract was filtered through Celite. Evaporation of the filtrate yielded 0.15 g, 74%, of a yellow residue that was extremely soluble in hydrocarbon solvents. The slow evaporation of a solution of **6** in hexanes resulted in a 50 mg quantity of crystals suitable for X-ray diffraction.

Anal. Calcd for $C_{28}H_{51}N_3P_2Si_4Zr$: C, 48.37 H, 7.39; N, 6.04. Found: C, 48.41; H, 7.52; N, 5.98. ^1H NMR (C_6D_6, 500 MHz): δ_H 8.03 (m, 4H, *o*-H), 7.09 (m, 6H, *o*/*p*-H phenyl), 1.75 (s, 9H, C(CH_3)$_3$), 1.20 (AB m's, 8H, ring CH_2), 0.34 (s, 6H, ring $SiMe_2$), 0.33 (s, 6H, ring $SiMe_2$). $^{31}P\{^1H\}$ NMR (C_6D_6): δ_P −15.5 (s).

X-ray Crystallographic Analyses of 1, 3, 4, and 6. Crystallographic data appear in Table 1. The final unit-cell parameters were obtained by least-squares methods on the setting angles for 25 reflections with 2θ = 18.0−24.8° for **1**, 15.0−26.3° for **3**, and 17.1−22.5° for **4** and 11 949 reflections with 2θ = 5.0−55.8° for **6**. The intensities of three standard reflections, measured every 200 reflections throughout the data collections for **1**, **3**, and **4**, remained constant for **1** and decayed linearly by 1.8% for **3** and by 4.4% for **4**. The data were processed[55] and corrected for Lorentz and polarization effects and absorption (empirical, based on azimuthal scans for **1**, **3**, and **4** and symmetry analysis of redundant data using 4th order spherical harmonics for **6**).

The structures were all solved by the Patterson method. The structure analysis of **3** was initiated in the centrosymmetric space group *C*2/*c* on the basis of the *E*-statistics, this choice being confirmed by the subsequent successful solution and refinement of the structure. The asymmetric unit of **3** consists of two crystallographically independent half-molecules lying on 2-fold axes and one molecule in a general position. There is considerable thermal motion in **3** at room temperature, peripheral atoms in general displaying high thermal motion. All non-hydrogen atoms were refined with anisotropic thermal parameters. Hydrogen atoms were fixed in idealized positions (methyl groups staggered, C−H = 0.98 Å, B_H = 1.2 $B_{\text{bonded atom}}$). A correction for secondary extinction was applied for **1**, the final value of the extinction coefficient being 5.42(12) × 10^{-7}. No extinction corrections were necessary for the three other complexes. Neutral atom scattering factors for all atoms and anomalous dispersion corrections for the non-hydrogen atoms were taken from ref 56. The absolute configuration of **1** (for the particular crystal used) was determined by parallel refinement of the mirror images. The *R* and *R*w factor ratios were 1.021 and 1.027, respectively. Selected bond lengths and bond angles appear in Tables 2−5. Atomic coordinates, anisotropic thermal parameters, complete bond lengths and bond angles, torsion angles, intermolecular contacts, and least-squares planes are included as Supporting Information.

Acknowledgment. Funding for this research was generously provided by the NSERC of Canada.

Supporting Information Available: Full experimental details, tables of X-ray parameters, fractional coordinates and thermal parameters, bond lengths, bond angles, and torsion angles, and ORTEP diagrams for compounds **1**, **3**, **4**, and **6** (73 pages). Ordering information is given on any current masthead page.

OM9707984

(55) *teXsan*: *Crystal Structure Analysis Package*; Molecular Structure Corp.: The Woodlands, TX, 1995.

(56) (a) *International Tables for X-Ray Crystallography*; Kynoch Press: Birmingham, U.K. (present distributor Kluwer Academic Publishers, Boston, MA), 1974; Vol. IV, pp 99−102. (b) *International Tables for Crystallography*; Kluwer Academic Publishers: Boston, MA, 1992; Vol. C, pp 200−206.